minerals

MDPI

Article

Characteristics of Laterite Soil for Potential Geopolymer Applications

Zeyneb K. Nuru [1,*], Walied A. Elsaigh [1] and Elsabe P. Kearsley [2]

[1] Department of Civil & Environmental Engineering and Building Science, University of South Africa, Johannesburg 1710, South Africa; hussiwam@unisa.ac.za
[2] Department of Civil Engineering, University of Pretoria, Pretoria 0002, South Africa; elsabe.kearsley@up.ac.za
* Correspondence: 17460069@mylife.unisa.ac.za

Abstract

Laterite soil is widely found in various tropical and subtropical regions. This study focuses on the physical and chemical properties of laterite soil as a precursor for geopolymer synthesis. The characteristics of the soil were determined through experimental analyses, including XRF, XRD, SEM, EDS, FTIR, TGA/DTA, and pH measurements. XRF analysis revealed that the primary chemical oxides are silica, alumina, and iron oxide, which are very essential for geopolymer production. Both XRD and FTIR assessments revealed that the calcination process applied to laterite diminishes its crystallinity while enhancing its amorphous nature, thereby improving its reactivity. TGA and DTA results confirmed significant weight loss and dihydroxylation between 400 °C and 700 °C, while temperatures above 700 °C showed minimal weight loss and no further dihydroxylation. The pH of the tested laterite soil was measured at 5.35, indicating strong acidic behaviour. Based on these combined chemical and physical analyses, this study concludes that laterite soil is a viable precursor material for geopolymer synthesis.

Keywords: laterization; laterite soil; chemical properties; microstructural properties; mineralogical analysis; geopolymer precursor

Academic Editors: Manuel Pozo Rodríguez and Alexander Mikhailovich Kalinkin

Received: 13 May 2025
Revised: 30 June 2025
Accepted: 2 July 2025
Published: 9 July 2025

Citation: Nuru, Z.K.; Elsaigh, W.A.; Kearsley, E.P. Characteristics of Laterite Soil for Potential Geopolymer Applications. *Minerals* **2025**, *15*, 719. https://doi.org/10.3390/min15070719

1. Introduction

The term lateritic was first employed by Francis Buchanan Hamilton in 1807 to describe the nature of the soil available in the mountain region of Malabar, India. Laterite was easily utilized as construction material in the form of blocks [1]. The word "laterite" is derived from the Latin word "later", meaning brick [2]. Laterite soils are widely available throughout the world, particularly in Africa, India, and Australia [3]. They are predominantly found in environments that have undergone leaching and oxidation, resulting in a distinct reddish or yellowish colour. These soils are underlain by cemented gravels, which consist of goethite, hematite, quartz, and kaolinite [4]. In general, it is formed where the parent rock is rich in silica, alumina, and iron [5].

Laterites and lateritic terms are often used interchangeably to name soils that are found in the tropical and subtropical climatic regions, and which are produced through an intensive weathering process called laterization. The degree of laterization varies according to the weather conditions, such as rainfall and temperature. The classification of laterite soil by Martin, 1927 [6], was based on physical properties. It was further suggested that if the ratio of silica to alumina in the clay is between 2.0 and 1.33, the soil should be described as "lateritic", and where this ratio falls below 1.33, the soil should be described as laterite.

However, this classification was criticized by Pendelton and Sharasuvana [7], indicating that both criteria are not enough for classification, and they further suggested considering the morphological characteristics of the laterite profile. In the study by Lyle & John [5], it was found that the chemical composition of laterite has no constant demarcation; it varies based on the parent rock formation. According to the study on Australian laterite by Mahalinga-Iyer and Williams [8], soil with a ratio of silica-to-sesquioxide equal to 2.5 can be classified as laterite, due to the presence of more quartz gravel; hence, it has a relatively high silica content.

The physicochemical behaviour of laterites is influenced by climatic–vegetational zones, parent rocks, genetic soil, the degree of leaching and laterization, and clay content [9]. Therefore, according to the study by Lyle & John [5], the morphological, chemical, and mineralogical characteristics of laterite soils in the African continent have wide ranges. This was confirmed by Mahalinga-Iyer and Williams [10], indicating that the mineralogy and microstructure of lateritic soil differ significantly from one geographical location to another.

Recent studies show that laterite soils are one of few promising precursor materials in synthesizing geopolymers [11–13]. Alkali solutions were used to dissolve the chemical composition of the precursor and produced relatively strong geopolymer matrices [14]. Calcination is an essential technique that is used to increase the reactivity of laterite soil in the geopolymer cement manufacturing process. According to the investigations on laterite precursor soils by Poudeu et al. [15] and Metekong et al. [16], the polycondensation of laterite-based geopolymer increases at calcination temperatures between 550 °C and 750 °C. Furthermore, Kakali et al. [17] found that the calcination of kaolinite material results in disruption to its structure, decreasing crystallinity, resulting in an amorphous phase, and ultimately causing increased reactivity. Similarly, Davidovits [18] explained how heating laterite soils can convert clay minerals, especially kaolinite, into metakaolinite. This transformation allows chemical compounds to dissolve more effectively when mixed with an alkaline activating agent. The resulting geopolymer cement demonstrates excellent mechanical and physical properties [14]. In addition, the recent study by Nuru et al. [19] reported that laterite soil calcined at 700 °C for 4 h achieved a 28-day compressive strength of 51 MPa.

Although some researchers have examined certain characteristics of laterite soil, its chemical behaviour varies depending on the source of the soil, e.g., the geographical location. Furthermore, there is limited research on its potential as a geopolymer precursor. The aim of this paper is to investigate the potential of laterite as a geopolymer precursor by determining the characteristics of both raw and calcined laterite found in Johannesburg, South Africa, including their physical and chemical properties.

2. Materials and Analytical Techniques

This study investigates the physical and chemical properties of laterite soil in both its raw and calcined forms, with a particle size below 150 µm. To achieve this, six characterization techniques were employed. The collected soil was first oven-dried at 105 °C for 24 h to remove moisture, then pulverized and sieved to obtain a uniform particle size of 150 µm. Calcination was performed in a muffle furnace under ambient air conditions. Based on previous experimental findings [11], the soil was calcined at 700 °C for 4 h to activate its reactive phases.

2.1. X-Ray Fluorescence (XRF)

The chemical composition of raw laterite powder was determined using an ARL Perform'X Sequential XRF Spectrometer, with Uniquant software employed for analysis.

The software analyzes all elements in the periodic table from sodium (Na) to uranium (U), but only reports on elements that are present at significant levels.

2.2. X-Ray Diffraction (XRD)

The mineralogical analysis of the laterite sample was performed by preparing it for X-ray diffraction (XRD) analysis through the backloading method. Diffractograms were obtained with a Malvern Panalytical Aeris diffractometer, which features a PIXcel detector and fixed slits, utilizing Fe-filtered Co-Kα radiation. The scanning was performed at a speed of 8 min per degree 2θ. Phase identification was conducted using X'Pert High Score Plus software in conjunction with the PAN-ICSD database. Relative phase quantities (weight%) were estimated through the Rietveld Refinement method, allowing for both qualitative and quantitative analysis.

2.3. Scanning Electron Microscopy (SEM) and Energy-Dispersive X-Ray Spectroscopy (EDS)

The laterite soil powder, both raw and calcined, was used for microstructural observations with a 6010 PLUS/LA-JEOL Scanning Electron Microscope (SEM) equipped with an Oxford Energy Dispersive X-Ray Spectroscopy (EDS) system manufactured by Rikagu, Tokyo, Japan. The samples were initially mounted in epoxy moulds, polished, and then carbon-coated prior to the SEM and EDS analysis. The examination was conducted using a backscatter electron detector at an acceleration voltage of 15 kV and a working distance of approximately 8 mm.

2.4. Fourier Transform Infrared Spectroscopy (FTIR)

The Attenuated Total Reflectance Fourier Transform Infrared Spectroscopy (ATR-FTIR) technique was employed to identify the main chemical groups present in both raw and calcined laterite soil. The study utilized a Vertex 70v FT-IR Spectrometer from Bruker Optics, Billerica, MA, USA. The sample was placed in the apparatus for characterization, and acquisitions were recorded between 400 cm^{-1} and 4000 cm^{-1}. The resulting data were processed using Origin Pro 8.1 software.

2.5. Thermogravimetric (TGA) and Differential Thermal (DTA) Analyses

TGA and DTA measurements were performed simultaneously using the TGA/DSC SDT Q600 Thermogravimetric Analyzer with TA software, also known as TA Instruments, manufactured in New Castle, DE, USA. The raw laterite and calcined samples were run in a random order and analyzed in a platinum crucible. The experiments were conducted between 30 °C and 1200 °C at a rate of 20 °C/min with a nitrogen purge.

2.6. pH Test

Determining the pH of the laterite precursor is crucial for understanding its reactivity. This eventually helps to adjust the amount of activator needed in the production of geopolymer products. The raw and calcined laterite samples were dispersed in deionized water (i.e., solvent) at a solid-to-solvent ratio of 1:5 [20]. The pH device was calibrated with buffer solutions of pH 4 and pH 7 prior to testing. To protect any interaction between the specimen solution and the surrounding environment, pH measurements were performed within one hour of sample preparation. The pH was measured using a benchtop pH meter equipped with a combination glass electrode containing an Ag/AgCl reference and a 3.0 M KCl internal solution under ambient temperature conditions with automatic temperature compensation.

3. Results and Discussion

3.1. XRF

The primary oxides of laterite soil are presented in Table 1. The oxides in notable percentages are silicon dioxide (SiO_2), aluminum oxide (Al_2O_3), and iron oxide (Fe_2O_3), which together account for approximately 87.7% of the soil's composition, which qualifies the laterites as class (F) pozzolan, according to criteria presented in ASTM C-618-1 [21]. The ratio of silica to alumina in the tested laterite is 3.05. This relatively high ratio attributes to the presence of high amount of quartz particles in the laterite. Furthermore, the ratio of 3.05 can be linked to acidic conditions that may prevail within the soil source area. This leads to the leaching out of alumina while silica remains. According to Townsend [22], when the ratio of SiO_2 to Al_2O_3 increases, the chemical reactivity, in terms of the geopolymerization, also increases, especially in the presence of amorphous materials. This enhancement in reactivity makes it promising for use in geopolymer synthesis. The chemical composition of the laterite soil is consistent with the findings of Abomo et al. [23], who identified it as a suitable precursor for geopolymer production. The loss of ignition (8.54%) is relatively high and is indicative of the presence of organic materials. It is worth pointing out that the presence of organic materials may impact adversely on the geopolymeriztion reaction; hence, calcination is necessary.

Table 1. Oxide composition of raw laterite soil.

Oxide	Mass (%)	Oxide	Mass (%)
SiO_2	61.09	MnO	0.04
Al_2O_3	20.04	P_2O_5	0.04
Fe_2O_3	6.64	Nb_2O_5	0.03
K_2O	1.92	Cr_2O_3	0.02
MgO	0.67	V_2O_5	0.01
TiO_2	0.57	Na_2O	<0.01
ZrO_2	0.18	LOI	8.54
CaO	0.09		

3.2. XRD Analysis

Figure 1 presents the XRD patterns of the raw and calcined laterite soil sample, while Table 2 shows the percentage of minerals in the laterite soil. The XRD data regarding the constituent minerals was derived according to the PAN-ICSD database. The main constituent minerals of raw laterite are quartz (O_2Si_1), albite ($Al_{1.02}Ca_{0.02}Na_{0.98}O_8Si_{2.98}$), kaolinite ($H_4Al_2O_9Si_2$), and muscovite ($H_2Al_3K_1O1_2Si_3$). In addition, the tested laterite contains a detectable amount of microcline ($Al_1K_1O_8Si_3$). After the soil is subjected to calcination, the mineralogical composition changes in both presence and amount. The amount of quartz (O_2Si_1) is slightly reduced, while the amounts of microcline ($K_1Al_1Si_3O_8$) and muscovite ($H_{1.828}Al_{2.472}F_{0.172}Fe_{0.315}K_1O_{11.828}Si_{3.28}$) increase. New minerals, such as hematite (Fe_2O_3) and biotite ($H_{2.548}Al_{2.432}Fe_{2.427}K_{1.891}Mg_{3.09}Mn_{0.035}Na_{0.062}O_{24}Si_{5.568}Ti_{0.448}$), are also observed. Kaolinite is no longer present in the soil, which can be attributed to its transformation into metakaolin [24]. According to Carvalheiras et al. [25], the amorphous hump between 15° and 35° 2θ is indicative of meta-kaolinite presence; however, it is not distinctly visible. This may be due to the dominant presence of crystalline phases such as quartz. The appearance of biotite is linked to the transformation of magnesium and potassium oxides, although these are present in trace amounts in the soil. The emergence of hematite seems to result from the transformation of goethite during the heating process [15]. Furthermore, the XRD patterns shown in Figure 1 indicate the existence of quartz and muscovite after and before calcination, meaning that their presence had not changed due to the thermal

treatment. However, all the mineral peaks were reduced, suggesting a crystallinity reduction, as is also evident in the FTIR analysis presented in a later section of this paper. The absence of kaolinite peaks and reduction in the peak intensity support the formation of an amorphous, reactive aluminosilicate phase. The experimental results confirm that thermal treatment leads to significant structural transformations, making the material suitable for geopolymer production.

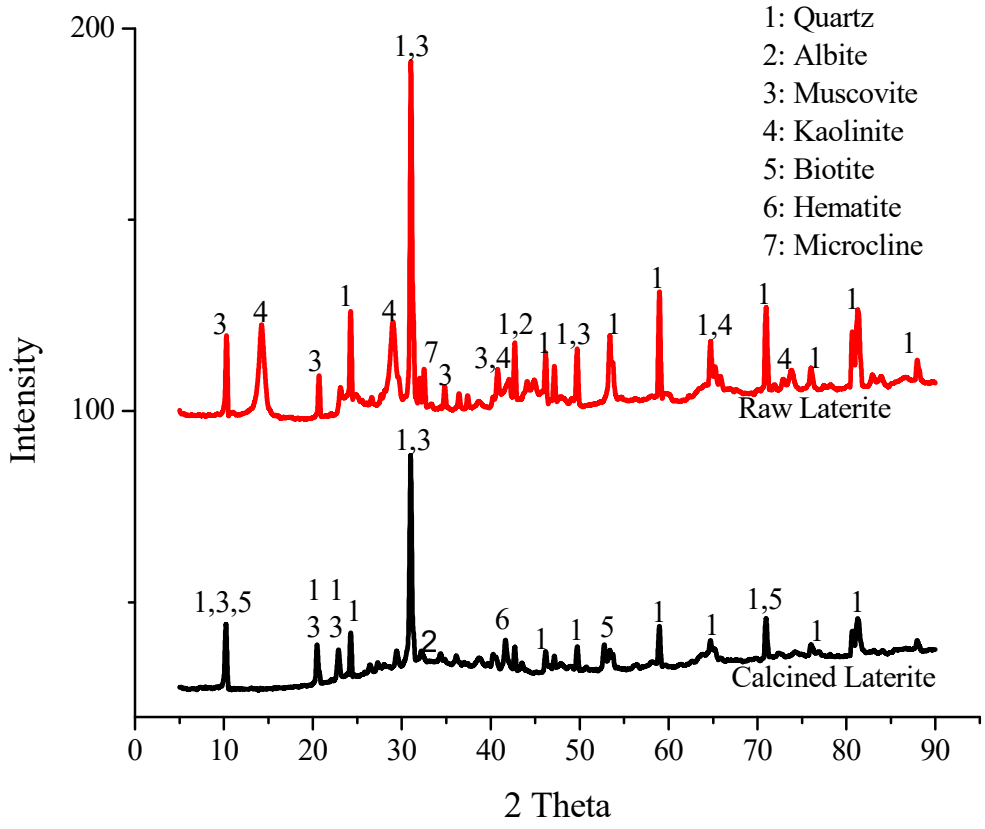

Figure 1. XRD Analysis of raw and calcined laterite.

Table 2. Mineralogical composition of raw laterite (LN) and calcined laterite (LC) (weight percent, *w*/*w*).

	Quartz	Albite	Microcline	Muscovite	Kaolinite	Biotite	Hematite
LN	52.1	4	0.7	14.6	28.6	-	-
LC	49.9	0.0	9	24.9	-	5.5	10.7

3.3. SEM and EDS Analysis

Figure 2a,c display micrographs of raw and calcined laterite soils. It was observed that the calcined laterite exhibits a clearer image of particle size and shape compared to the raw sample. The image in Figure 2a,c shows the shapes of the laterite soil before and after calcination, respectively. The calcined laterite appears to be angular in shape, while raw laterite exhibits flaky and elongated shapes. This means that calcined laterite will pack more closely, leaving less voids as compared to raw laterite. It should bear in mind that the packing density will influence the final geopolymer product. Additionally, the calcined sample micrograph reveals a reduction in particle size, which may be attributed to the transformation from being crystalline to the amorphous phase, and the removal of organic particles. The finer fraction of laterite exhibits greater reactivity due to the presence of amorphous materials [26]. This result is consistent with the study by Metekong et al. [16], which

showed that the application of heat to the laterite resulted in the formation of finer particles and the creation of an amorphous phase due to the physicochemical transformations occurring during the calcination process.

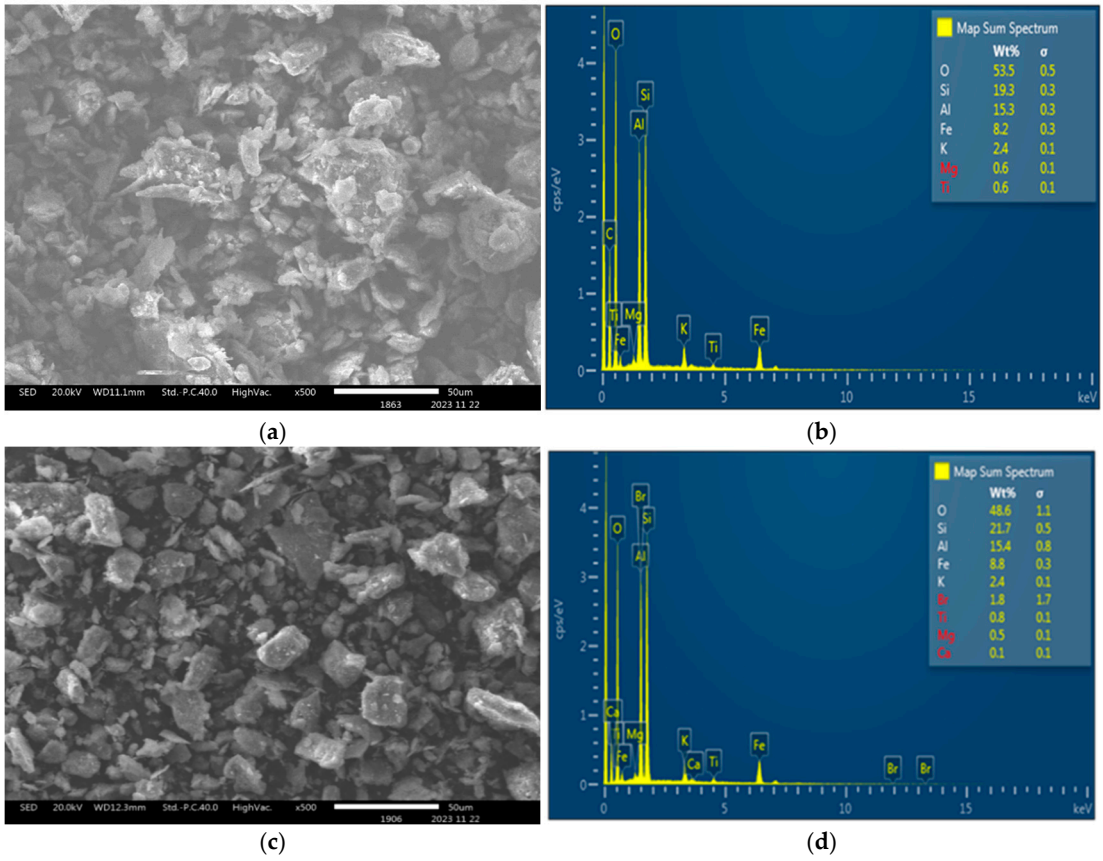

Figure 2. SEM and EDS analysis of raw and calcined laterite. (**a**) SEM image—raw laterite. (**b**) EDS Spectra—raw laterite. (**c**) SEM image—calcined laterite. (**d**) EDS spectra—calcined laterite.

Refer to the results of EDS analysis presented in Figure 2b,d; carbon was detected in the raw laterite, which relates well to the LOS results presented in Table 1. However, in the calcined laterite, carbon was not detected. This could possibly be a result of organic material decomposition due to thermal treatment. Furthermore, the number of other elements present in the laterite showed slight change. The silica, alumina, and iron content were increased after the calcination, while oxygen was reduced, and potassium remained unchanged. In general, temperature had an influence on the physicochemical properties of laterite soil.

3.4. FTIR Analysis

In the FTIR analysis shown in Figure 3, distinctive features of raw laterite can be observed. According to the studies by Poudeu et al. [15] and Tantono et al. [14], the peaks in the band between 3705 and 3627 cm^{-1} indicate the presence of a OH group of Si, Al, and Fe which is assigned to the stretching bond and an axial symmetric mode of kaolinite: goethite. The study by Ghani et al. [27], explained that the band at 910 cm^{-1} relates to OH bending vibration in the presence of kaolinite. Poudeu et al. [15] and Mimboe et al. [28] confirmed that the band at 1007 cm^{-1} is assigned to the symmetrical stretching vibration of Si-O-(Al, Si, Fe). Other bands, such as the Fe-OH bending vibration bands observed at 684 cm^{-1}, confirm the presence of goethite, according to Mimboe et al. [28], while the peaks at 533 cm^{-1} and 437 cm^{-1} are assigned to bending vibrating bonds of Al-O-Si and Fe-O-Si bonds by [29].

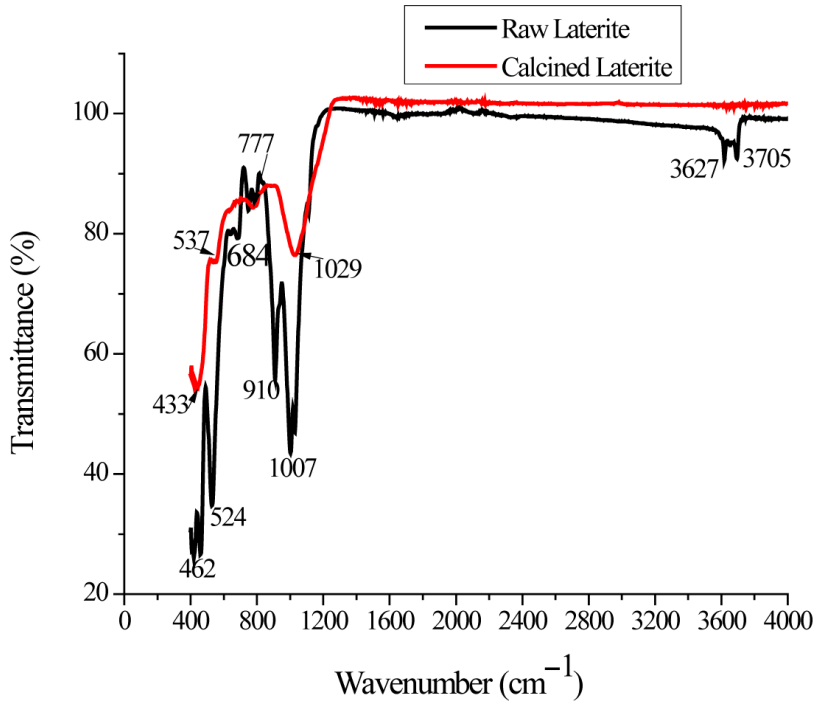

Figure 3. FTIR analysis of raw and calcinated laterite.

After the laterite was calcined at 700 °C for 4 h, changes in the spectrum were observed. The bands at 3705 and 3627 cm^{-1} disappear, indicating the complete dehydroxylation of the OH chemical group into the calcined laterite. The disappearance of the peak at 910 cm^{-1} confirms the removal of the OH bending vibration of Kaolin. The disappearance of the band at 684 cm^{-1} was also observed. According to Bewa et al. [30] and Tantono et al. [14], the disappearance of the band is due to the dihydroxylation of goethite (Fe-OH). In the study by Tantono et al. [14], the band at 777 cm^{-1} was attributed to the deformed vibration of the Si–O bond, indicating the presence of amorphous silica. Additionally, there was a decrease in the intensity of the absorption bands at 537 cm^{-1} and 433 cm^{-1}, and the appearance of new broad bands at 1029 cm^{-1}. According to the authors Mimboe et al. [28], Kakali et al. [17], and Barbosa et al. [31], this band corresponded to the Si–O stretch vibration bond that transitioned from crystallinity to an amorphous phase.

3.5. TGA and DTA Analysis

Figure 4 presents the TGA and DTA curves of raw laterite. The DTA thermogram exhibits three endothermal the peaks, which are located at 30–110 °C, 240–340 °C, and 400–700 °C. The first interval, the spanning peak, observed between 30 and 110 °C, is attributed to the loss of free water or the removal of water from the material's cavities. This water loss explains the corresponding 0.9% mass loss observed in the TGA curve. The second peak, occurring between 240 and 340 °C, corresponds to the process of dihydroxylation and the conversion of goethite into hematite [32,33], resulting in a recorded mass loss of 0.85%. The final interval of the third peak falls within the range of 400–700 °C and involves the dihydroxylation of kaolinite to form reactive metakaolinite [23,34]. This suggests that the thermal treatment of laterite soil at 700 °C has a positive impact in relation to the potential for geopolymer synthesis. This process is accompanied by a recorded weight loss of 7.7% in the TGA curve.

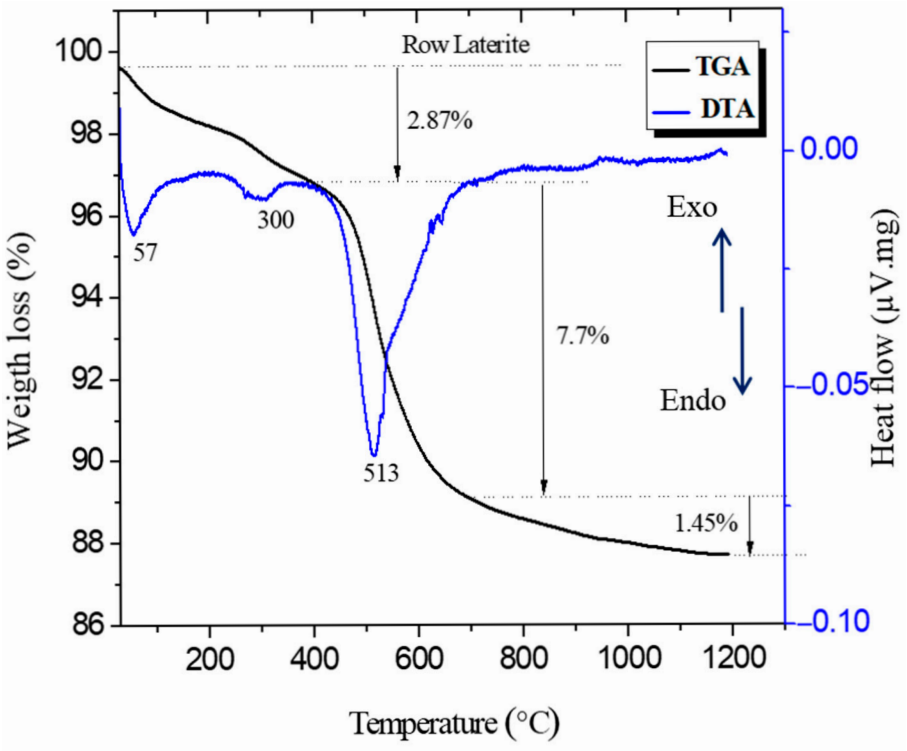

Figure 4. TGA and DTA curves of raw laterite.

3.6. pH of Laterite Soil

The hydrogen potential (pH) value of the raw laterite is recorded at 5.35, categorized under a strong acidic condition [35], which may be attributed to its low content of calcium oxide (0.09%), sodium oxide (<0.01), and potassium oxide (1.92%); refer to Table 1. Therefore, the results suggest that a strong alkali activator is needed to assist in the decomposition of the aluminosilicate composition and to enhance reactivity in producing a geopolymer gel, leading to high strength.

The findings correlate well with the findings of other studies on the pH requirements for the geopolymerization process to happen. The study by Anburuvel [36] found that the recommended pH values for geopolymerization range between 10 and 13, as this facilitates the dissolution of silica and alumina in the precursor materials, allowing them to react and form a geopolymer matrix. Khale and Chaudhary [37] also confirmed that higher pH values, from 13 to 14, exhibit greater compressive strength in geopolymer concrete. For fly ash as a precursor material, pH values from 8 to 11 were attributed to the high content of calcium oxide [38]. In their investigation, pH increased to 13 when the alkali solution (NaOH) concentration was increased from 0.5 to 6 M. In another study on fly ash, Saride and Jallu [39] found that a pH of 12 can be obtained by a smaller increase in the NaOH concentration from 0.5 to 3 M. The reason for this could be the difference in the composition of the fly ash used.

4. Conclusions

Based on the experimental study of the chemical and microstructural characterization of laterite soil, it can be concluded that laterite soil serves as a promising, efficient precursor material for geopolymer synthesis.

The XRF results indicate that the main chemical oxides present in the laterite soil are silica, aluminum oxide, and iron oxide, alongside a high silica-to-alumina ratio. The EDS analysis confirms that the presence of organic matter necessitates the calcination of the soil before it can be used as a precursor to reduce unreactive minerals during mixing.

The SEM image reveals that after calcination, the laterite particles become more angular in shape, and the reduction in particle size indicates a higher packing density and increased reactivity when incorporated into geopolymer synthesis.

XRD analysis reveals the mineralogical composition of laterite in its raw and calcined state. The amount of quartz decreases, kaolinite completely disappears, and new minerals appear, indicating a phase change. The FTIR analysis further confirms that the chemical composition changes with temperature, resulting in complete dihydroxylation. This finding supports that laterite soil, after heat treatment, decreases crystallinity and increases the reactivity of the aluminosilicate material.

TGA and DTA curve results show a major weight loss recorded at temperatures ranging from 400 to 700 °C due to the dihydroxylation process. It is concluded that chemical compound decomposition occurs at 700 °C, and hence this is used as the calcination temperature.

The pH value of the precursor material seems to influence the result of geopolymer synthesis. This suggests that a strong alkaline activator is required to boost the pH to allow for the silica and alumina to dissolve, hence producing a strong geopolymer matrix.

It is worth noting that the chemical composition of laterite soils can vary significantly depending on factors such as the parent rock, climate, degree of weather, and regional geology. However, most laterite soils, regardless of origin, share common characteristics: high Fe_2O_3, Al_2O_3, and SiO_2 contents, and low CaO and MgO. In this study, the laterite used was characterized thoroughly, and its chemical profile aligns with the general properties reported in the literature from other tropical and subtropical regions. Nevertheless, the results from this study may not be directly transferable to all laterite sources without further local characterization.

Author Contributions: Z.K.N.: Conceptualization, Investigation, Methodology, Data curation, Formal analysis, Writing—original draft. W.A.E.: Supervision, Investigation, Validation, Visualization, Formal analysis, Writing—review and editing. E.P.K.: Supervision, Validation, Visualization and Writing—review and editing. All authors have read and agreed to the published version of the manuscript.

Funding: University of south Africa, CSET bursary.

Data Availability Statement: The original contributions presented in this study are included in the article. Further inquiries can be directed to the corresponding author.

Acknowledgments: The author would like to thank the University of South Africa's College of Science, Engineering, and Technology, the Civil Engineering and Chemistry Departments, as well as the iNanoWS Science Campus in Johannesburg, South Africa.

Conflicts of Interest: The author declares no conflicts of interest or competing interests related to this manuscript.

References

1. Buchanan, F.H. *A Journey from Madras Through the Countries of Mysore, Canara, and Malabar*; Cadell, T., Davies, W., Eds.; Black, Parry, and Kingsbury: London, UK, 1807; Volume 3.
2. Thurston, E. *The Madras Presidency with Mysore, Coorg and the Associated States, Provincial Geographies of India*; Cambridge University Press: London, UK, 1913; Volume 1.
3. Maignien, R. *Review of Research on Laterites*; Natural Resources Research IV; The United Nations Education, Scientific and Cultural Organization Vaillant-Carmanne: Paris, France, 1966; Volume 4, pp. 1–156.
4. Kheoruenromne, I.R.B. Red and Yellow Soil and Laterite Formation in the Northeast Plateau, Thailand. *Chem. Geol.* **1987**, *60*, 319–326.
5. Lyle, A.; John, C. *Genesis and Hardening of Laterite in Soils*; US Department of Agriculture: Washington, DC, USA, 1962; Volume 1282.

6. Martin, F.J.; Doyne, H.C. Laterite and Lateritic Soils in Sierra Leone. *J. Agric. Sci.* **1927**, *17*, 530–547. [CrossRef]
7. Pendleton, R.L.; Sharasuvana, S. Analyses of Some Siamese Laterites. *Soil. Sci.* **1946**, *62*, 423–440.
8. Mahalinga-Iyer, U.; Williams, D.J. Properties and Performance of Lateritic Soil in Road Pavements. *Eng. Geol.* **1997**, *46*, 71–80.
9. Gidigasu, M.D. The Importance of Soil Genesis in the Engineering Classification of Ghana Soils. *Eng. Geol.* **1971**, *5*, 117–161.
10. Mahalinga-Iyer, U.; Williams, D.J. Engineering Properties of a Lateritic Soil Profile. *Eng. Geol.* **1991**, *31*, 45–58.
11. Nuru, Z.K.; Kearsley, E.P.; Elsaigh, W.A.; Student, P.D. Application of Laterite-Based Geopolymer Mortar for Masonry Bedding. *Mater. Sci. Forum* **2024**, *1137*, 81–86. [CrossRef]
12. Kaze, R.C.; Lemougna, P.N.; Alomayri, T.; Assaedi, H.; Adesina, A.; Kumar Das, S.; Lecomte-Nana, G.L.; Elie, K.; Melo, U.C.; Cristina, L. Characterization and Performance Evaluation of Laterite Based Geopolymer Binder Cured at Different Temperatures. *Constr. Build. Mater.* **2021**, *270*, 121443. [CrossRef]
13. Subaer; Haris, A.; Irhamsyah, A.; Akifah, N.; Amalia, N.S. Physico-Mechanical Properties of Geopolymer Based on Laterite Deposit Sidrap, South Sulawesi. *J. Phys. Conf. Ser.* **2019**, *1244*, 012037.
14. Tantono, S.N.; Belibi Belibi, P.D.; Baenla, J.; Elimbi, A. Alkaline and Acid Activations of Calcined Laterites: A Comparative Study. *Silicon* **2023**, *15*, 2797–2810. [CrossRef]
15. Poudeu, R.C.; Ekani, C.J.; Djangang, C.N.; Blanchart, P. Role of Heat-Treated Laterite on the Strengthening of Geopolymer Designed with Laterite as Solid Precursor. *Ann. Chim. Sci. Des. Mater.* **2019**, *43*, 359–367. [CrossRef]
16. Metekong, J.V.S.; Kaze, C.R.; Adesina, A.; Nemaleu, J.G.D.; Djobo, J.N.Y.; Lemougna, P.N.; Alomayri, T.; Kamseu, E.; Melo, U.C.; Tatietse, T.T. Influence of Thermal Activation and Silica Modulus on the Properties of Clayey-Lateritic Based Geopolymer Binders Cured at Room Temperature. *Silicon* **2022**, *14*, 7399–7416. [CrossRef]
17. Kakali, G.; Perraki, T.; Tsivilis, S.; Badogiannis, E. Thermal Treatment of Kaolin: The Effect of Mineralogy on the Pozzolanic Activity. *Appl. Clay Sci.* **2001**, *20*, 73–80.
18. Joseph, D. *Geopolymer Chemistry and Applications*, 5th ed.; Geopolymer Institute: Saint-Quentin, France, 2020; Volume 5, ISBN 9782954453118.
19. Nuru, Z.K.; Elsaigh, W.A.; Kearsley, E.P. The Influence of Curing Method on Properties of Laterite Soil Based Geopolymer Cement. *Constr. Build. Mater.* **2025**, *483*, 141768.
20. *ISO 10390*; Soil, Treated Biowaste and Sludge-Determination of PH. ISO: Geneva, Switzerland, 2021.
21. *ASTM C618-19*; Standard Specification for Coal Fly Ash and Raw or Calcined Natural Pozzolan for Use in Concrete. ASTM International: West Conshohocken, PA, USA, 2019.
22. Townsend, F.C.; Manke, P.G.; Parcher, J. V The Influence of Sesquioxides on Lateritic Soil Properties. Ph.D. Thesis, Oklahoma State University, Stillwater, OK, USA, 1970. Volume 374.
23. Abomo, T.; Cyriaque Kaze, R.; Cengiz, O.; Alomayri, T.; Pefouo Wilson, T.; Eko Robert, M.; Naghizadeh, A.; Kamseu, E. Impact of the Depth of a Lateritic Profile on the Physicochemical, Mechanical and Microstructural Properties of Geopolymer Binders. *Constr. Build. Mater.* **2023**, *403*, 133138. [CrossRef]
24. Elimbi, A.; Tchakoute, H.K.; Njopwouo, D. Effects of Calcination Temperature of Kaolinite Clays on the Properties of Geopolymer Cements. *Constr. Build. Mater.* **2011**, *25*, 2805–2812. [CrossRef]
25. Carvalheiras, J.; Novais, R.M.; Labrincha, J.A. Metakaolin/Red Mud-Derived Geopolymer Monoliths: Novel Bulk-Type Sorbents for Lead Removal from Wastewaters. *Appl. Clay Sci.* **2023**, *232*, 106770.
26. Townsend, F.C. *The Influence of Sesquioxides on Some Physico-Chemical and Engineering Properties of a Lateritic Soil*; Oklahoma State University: Stillwater, OK, USA, 1970.
27. Ghani, U.; Hussain, S.; Noor-ul-Amin; Imtiaz, M.; Khan, S.A. Role of Calcination on Geopolymerization of Lateritic Clay by Alkali Treatment. *J. Saudi Chem. Soc.* **2021**, *25*, 101198. [CrossRef]
28. Mimboe, A.G.; Abo, M.T.; Djobo, J.N.Y.; Tome, S.; Kaze, R.C.; Deutou, J.G.N. Lateritic Soil Based-Compressed Earth Bricks Stabilized with Phosphate Binder. *J. Build. Eng.* **2020**, *31*, 101465. [CrossRef]
29. Akhmal Saadon, S.; Rahim Mohd Yusoff, A.; Yusop, Z.; Azman, S.; Uy Achmad Syafiuddin, D. Heated Laterite as a Low-Cost Adsorbent for Arsenic Removal from Aqueous Solution. *Malays. J. Fundam. Appl. Sci.* **2018**, *14*, 1–8.
30. Bewa, C.N.; Tchakouté, H.K.; Rüscher, C.H.; Kamseu, E.; Leonelli, C. Influence of the Curing Temperature on the Properties of Poly (Phospho-Ferro-Siloxo) Networks from Laterite. *SN Appl. Sci.* **2019**, *1*, 1–12. [CrossRef]
31. Barbosa, V.F.; MacKenzie, K.J.; Thaumaturgo, C. Synthesis and characterisation of materials based on inorganic polymers of alumina and silica: Sodium polysialate polymers. *Int. J. Inorg. Mater.* **2000**, *2*, 309–317.
32. Song, X.; Boily, J.F. Surface and Bulk Thermal Dehydroxylation of FeOOH Polymorphs. *J. Phys. Chem. A* **2016**, *120*, 6249–6257. [CrossRef]
33. Lecomte-Nana, G.; Goure-Doubi, H.; Smith, A.; Wattiaux, A.; Lecomte, G. Effect of Iron Phase on the Strengthening of Lateritic-Based "Geomimetic" Materials. *Appl. Clay Sci.* **2012**, *70*, 14–21. [CrossRef]
34. Caballero, L.R.; de Moraes, E.; Fairbairn, R.; Dias, R.; Filho, T.; Civil, D.E.; de Janeiro, R. Thermal, Mechanical and Microstructural Analysis of Metakaolin Based Geopolymers 2. *Exp. Proced.* **2019**, *22*, 1–8.

35. Hughes, B.; Davenport, D.; Dohle, L. *Standard Soil Test Methods and Guidelines for Interpretation of Soil Results*; Government of South Australia: Adelaide, Australia, 1996.
36. Anburuvel, A. The Role of Activators in Geopolymer-Based Stabilization for Road Construction: A State-of-the-Art Review. *Multiscale Multidiscip. Model. Exp. Des.* **2023**, *6*, 41–59.
37. Khale, D.; Chaudhary, R. Mechanism of Geopolymerization and Factors Influencing Its Development: A Review. *J. Mater. Sci.* **2007**, *42*, 729–746. [CrossRef]
38. Risdanareni, P.; Puspitasari, P.; Januarti Jaya, E. Chemical and Physical Characterization of Fly Ash as Geopolymer Material. In Proceedings of the MATEC Web of Conferences, Sibiu, Romania, 7–9 June 2017; EDP Sciences: Les Ulis, France, 2017; Volume 97.
39. Saride, S.; Jallu, M. Effect of Fly Ash Geopolymer on Layer Coefficients of Reclaimed Asphalt Pavement Bases. *J. Transp. Eng. Part. B Pavements* **2020**, *146*, 04020033. [CrossRef]